SOIL SCIENCE ANNUAL
2025, 76(4), 215241

https://doi.org/10.37501/soilsa/215241

Dynamics of soil hydraulic conductivity in response to incremental changes in sodium adsorption ratio: Evidence for soil structural hysteresis

Louadj Yacine[1*], Semar Ahcène[2], Belghemmaz Salah[1]

[1] University Ferhat Abbas Sétif-1, Faculty of Life and Natural Sciences, Department of Agronomic Sciences, Laboratory of Natural Biological Resources Valorization, 19137, Sétif, Algeria
[2] National Higher Agronomic School (ENSA), Department of Rural Engineering, Laboratory of Water Management in Agriculture, 16004, El Harrach, Algiers, Algeria

* Corresponding author: Louadj Yacine, pedologist899@gmail.com, +213773125744 ORCID iD: https://orcid.org/0000-0003-1738-1797

Received: 2025-03-26
Accepted: 2025-12-06
Published online: 2025-12-06
Associated editor: Piotr Gajewski

Keywords:

Soil sodicity
Hydraulic conductivity
Hysteresis
Sodium adsorption ratio
Soil structure
Reclamation strategies

Abstract

Soil sodification poses a significant threat to agricultural productivity, but the reversibility of sodicity-induced changes in soil hydraulic properties remains poorly understood. This study investigated the hysteresis in saturated hydraulic conductivity (Ks) of a clayey soil from the Algerian lower Cheliff plain under varying sodium adsorption ratio (SAR) conditions. Three SAR increment scenarios (±5, ±15, and ±30) were employed to quantify the magnitude and persistence of structural changes in response to sodification. The results revealed a strong hysteresis effect, with Ks decreasing by up to 75% as the SAR increased from 0 to 30, and showing limited recovery upon reduction of the SAR. A critical threshold was identified between SAR 10 and 15, where soil structural degradation accelerated significantly. The hysteresis effect was most pronounced in the ±5 increment scenario, indicating that gradual changes in soil sodicity resulted in more persistent structural alterations. A hysteresis index (HI) was introduced to quantify the degree of irreversibility in soil hydraulic properties, with values ranging from 0.24 to 0.83 across different SAR levels. These findings challenge the assumption of reversibility in current sodic soil reclamation models and highlight the need for preventive management strategies. This study offers crucial insights into the complex dynamics of soil structural changes under fluctuating sodicity, with significant implications for developing more effective strategies to manage and reclaim sodic soils in arid and semiarid regions.

1. Introduction

Soil hydraulic conductivity (SHC) refers to the ability of soil to transmit water under the influence of a hydraulic gradient. SHC is dependent on the characteristics of the pores and percolating liquid (Hillel, 2004); furthermore, this parameter is associated with soil structure through two primary attributes: pore space geometry and structural stability (Ben-Hur et al., 2009). Extensive research has demonstrated that the chemical composition of percolating solutions affects the pore architecture, thereby influencing SHC (McNeal and Coleman, 1966; Frenkel et al., 1978; Daoud, 1993; Quirk, 2001; Levy et al., 2005). This relationship becomes particularly significant in arid and semi-arid regions, where soil salinization is frequently accompanied by sodification (Daoud, 1993).

Sodic soils, defined by an Exchangeable Sodium Percentage (ESP) exceeding 15% or a Sodium Adsorption Ratio (SAR) greater than 13, exhibit distinct physical and chemical properties that present significant challenges in both environmental and agricultural contexts. These soils are prone to poor structural integrity, which leads to issues such as clay dispersion, surface crusting, and notably reduced infiltration rates (Rengasamy, 2018). The environmental impacts of sodification are not limited to decreased agricultural productivity; they also include heightened erosion risks, diminished groundwater recharge, and increased sedimentation in surface water bodies (Demo et al., 2025). In regions where irrigation is practiced, the emergence of sodicity can initiate a positive feedback mechanism. This mechanism involves diminished infiltration, which necessitates more frequent irrigation, thereby potentially intensifying salt accumulation (Minhas and Qadir, 2024).

Soil structural degradation is the primary response to excess exchangeable sodium and low salinity (Oster and Shainberg, 2001; Mukhopadhyay et al., 2019). While the United States Salinity Laboratory (USSL, 1954) estimated the threshold for soil structure sensitivity to exchangeable sodium at 15%, subsequent

studies have shown that this threshold can be lower, depending on the saline concentration and other intrinsic soil factors (Sumner, 1993; Mace and Amrhein, 2001; Rengasamy and Marchuk, 2011; Bennet et al., 2019).

A landmark paper by Quirk and Schofield (1955) demonstrated that SHC decreases as the Sodium Adsorption Ratio (SAR) of the percolating solution increases, particularly when the saline concentration falls below a certain threshold. This threshold, defined as the saline concentration at which SHC drops by 15% due to exchangeable sodium, varies according to intrinsic factors such as soil texture, clay mineralogy, organic matter (OM) content, pH, and cementing agents like $CaCO_3$ and sesquioxides of iron and aluminum (Qadir and Schubert, 2002; Keren and Ben-Hur, 2003; Tavakkoli et al., 2015; Klopp and Daigh, 2019).

The mechanisms responsible for soil structural changes under the effect of sodic conditions are the dispersion of soil colloids and swelling of clays. The swelling of clay particles reduces the size of the conducting pores; conversely, the dispersion and migration of clay particle blocks the pores (Frenkel et al., 1978). A distinction should be made between the effect of swelling and clay dispersion on the evolution of SHC in sodic conditions. The soil begins to swell when the saline concentration of the soil solution is low, and the SAR is greater than or equal to 10 (Levy et al., 1999). Swelling is difficult to detect in sandy soils; conversely, soil dispersion occurs at all levels of SAR when the saline concentration is below the critical saline concentration or flocculation concentration of clay minerals in the soil (Levy and Shainberg, 2005). Keren and Ben-Hur (2003) demonstrated that soil swelling is a continuous process that increases progressively as the electrolyte concentration decreases and the sodium adsorption ratio (SAR) increases; on the other hand, soil dispersion is a rapid process that initiates when the saline concentration falls below the flocculation threshold of clay particles at a given SAR.

The interplay between salinity and sodicity in influencing colloid behavior is complex and critical for understanding the changes in saturated hydraulic conductivity. At high salinity levels, the abundance of electrolytes in the soil solution compresses the diffuse double layer surrounding clay particles, promoting flocculation and maintaining the soil structure (Sposito, 2008). As salinity decreased and sodicity increased, the diffuse double layer expanded, leading to increased repulsion between clay particles. This expansion manifests as swelling in 2:1 clay minerals such as montmorillonite or as dispersion when repulsive forces overcome attractive van der Waals forces (Oster and Shainberg, 1980; Sumner and Naidu, 1998). The reversibility of these processes is not straightforward and depends on various factors. Although swelling is generally considered a more reversible process, complete reversal may be hindered by hysteresis effects related to the rearrangement of clay particles and OM during the swelling process (Alperovitch et al., 1985). On the other hand, dispersion can lead to persistent changes in soil structure. Once dispersed, clay particles may migrate through the profile (Shainberg and Letey, 1984) and become lodged in soil pores, leading to pore clogging that may not be fully reversed, even when salinity is increased or sodicity is reduced (Ezlit et al., 2013;). Recent investigations have significantly enhanced our understanding of these complex soil mechanisms. Awdat et al. (2021) demonstrated, through a column study of saturated hydraulic conductivity, that the dispersion of clay particles and the subsequent clogging of pores in sodic soils exhibit distinct patterns contingent upon soil density and initial porosity. Specifically, soils with lower density exhibit a more pronounced reduction in hydraulic conductivity due to increased clay mobility through macropores. This finding offers direct visualization of the pore-scale processes that have long been hypothesized.

High concentrations of monovalent cations are known to break down bonds between soil particles, causing the dissolution of soil aggregates (McGeorge, 1954; Levy, 2011; Bardhan et al., 2016). Damage to soil aggregates restricts air and water movement of air and water in the soil's root zone, which in turn threatens plant growth (Mandal et al., 2008; Levy, 2011; Bardhan et al., 2016).

The reclamation of sodic soil is achieved by the addition of a calcium source (gypsum), which aims to replace exchangeable sodium with calcium (Ilyes et al., 1993). The primary objective of this process is to enhance the soil physical properties by promoting clay flocculation, improving soil structural stability, and increasing the infiltration rate (Lebron et al., 2002). From a chemical perspective, the substitution of Na^+ with Ca^{2+} in the soil exchange phase is considered a reversible process governed by the law of mass action and cation exchange equilibrium (Bolt, 1979; Essington, 2015). However, recent investigations have revealed a more complex scenario when the physical aspects of this exchange are taken into account. Notably, several studies have demonstrated a hysteresis effect in the exchange of Na^+ and Ca^{2+} ions, particularly in relation to the soil hydraulic properties (Dane and Klute, 1977; Mitchell and Donovan, 1991; Mace and Amrhein, 2001; Ezlit et al., 2013). This hysteresis phenomenon indicates that the physical response of the soil to alterations in ion composition is not entirely reversible. One potential explanation for this occurrence may include the entrapment of dispersed clay particles within pore spaces, thereby impeding the complete restoration of the original soil structure (Mitchell and Donovan, 1991; Mace and Amrhein, 2001; Ezlit et al., 2013). Recent research by Adeyemo et al. (2022) has provided new insights into the intricate relationship between salinity, sodicity, and saturated hydraulic conductivity. Their investigation demonstrated that modifications in saturated hydraulic conductivity (Ks) resulting from fluctuations in salinity and sodicity are not invariably reversible and exhibit hysteresis behavior.

Despite extensive research, the reversible nature of changes in SHC due to variations in salinity and sodicity remains unclear, particularly considering the observed hysteresis effects. This study aimed to address the significant gap in understanding the reversible nature of SHC changes under sodic conditions by investigating the effect of sodicity on the reversibility of SHC under non-saline conditions. Using the modified permeameter of McNeal and Reeve (1964), we targeted two primary objectives: i) to assess the effect of increasing SAR at a fixed EC (2 dS m^{-1}) with three different increments (+5, +15, and +30) on SHC; ii) and to evaluate the effect of decreasing SAR at a fixed EC (2 dS m^{-1}) with corresponding decreasing increments (–5, –15, –30) on the restoration of SHC, with particular attention to potential hysteresis effects.

2. Materials and methods

2.1. Site description and soil sample characterization

Soil samples were obtained at depths of 0–0.30 m from a region known as the Algerian lower Cheliff Valley, situated at latitude 36°10' N and longitude 00°30' to 1°20' E. A semi-arid climate, characterized by elevated temperatures in summer and low temperatures in winter, prevails in this area. The region experiences a mean annual precipitation of 350 mm and an average annual temperature of 18°C with minimal seasonal variations. The study site was located at an elevation of approximately 70 m above sea level. The soils in this area are pedologically young and have developed from alluvial parent material rich in clay and calcareous content (Saidi, 1985; Daoud, 1993). This alluvial origin contributes significantly to soil properties and classification (Saidi, 1985). The soil was classified as Typic Torrifluvent according to USDA (2014), and the main soil characteristics (Table 1) were provided by Laoufi (2010).

The soil sample was characterized using standard analytical procedures recommended by Mathieu and Pieltain (2003). Particle size distribution was determined using the pipette method; the cation exchange capacity (CEC) was measured using ammonium acetate at pH 7.0, while exchangeable sodium percentage (ESP) was calculated from the ratio of exchangeable sodium to CEC. The calcium carbonate (CaCO3) content was determined using the calcimeter method based on CO_2 evolution, and the soil pH was measured in a 1:2.5 soil-to-water suspension. As regards the determination of organic matter content, we used the Anne method, which involves the oxidation of organic carbon (Mathieu and Pieltain, 2003). Soil salinity was assessed by measuring electrical conductivity (EC) in a saturated soil paste extract.

The soil samples exhibited a mild alkalinity (pH 8.1). The soil composition consisted of 47% clay, 39% silt, and 14% sand, classified as a clayey textural class according to the USDA (2017) textural triangle. Using the standard pipette method to determine the distribution of different soil particles is subject to the risk of error due to either over- or under-estimation of clay or silt. According to Kobza et al. (2011) and Igaz et al. (2020), the accuracy of this method can reach 2.3%.

OM content was moderate (2.22%). The electrical conductivity (EC) and sodium adsorption ratio (SAR) of the saturated paste extract were 1.97 dS m^{-1} and 10.5, respectively, characterizing this sample as non-saline and slightly sodic. The calcium carbonate content was within the medium range. The cation exchange capacity (CEC) was 18.6 $cmol_c kg^{-1}$, and the exchangeable sodium percentage (ESP) was 11.63%. X-ray diffraction analysis revealed that the clay mineralogical composition comprised a mixture of interstratified smectite-illite (50%), kaolinite, vermiculite, and chlorite (Daoud, 1993). It is essential to acknowledge that these soil characteristics, as determined by Laoufi (2010), represent the initial condition of the soil utilized in our experiments. The clay mineralogy, specifically the interstratified smectite-illite, and the texture, comprising 47% clay, are particularly pertinent as they remain constant throughout our sodium-calcium exchange treatments. This constancy enables us to isolate the effects of changes in the Sodium Adsorption Ratio (SAR) on soil structure....

2.2. Saline and sodic solution preparation

In our study, the salinity was maintained at a constant level of 2 dS m^{-1} (20 $mmol_c L^{-1}$) to preserve the value of the soil salinity measurements, which was 1.97 dS m^{-1}. Conversely, sodicity, a critical variable, was quantified as the Sodium Adsorption Ratio (SAR), ranging from 0 to 30. This range indicates the extent of soil structure degradation due to exchangeable sodium, which was evaluated in our study through variations in the Ks. Furthermore, within this range, the SAR and Exchangeable Sodium Percentage (ESP) are numerically equivalent (US Salinity Laboratory Staff, 1954; Qadir and Schubert, 2002).

The Sodium Adsorption Ratio was calculated using the following formula:

$$SAR = Na^+ / (Ca^{2+} / 2)^{0.5} \quad \text{Equation 1}$$

Na^+ and Ca^{2+} were expressed in $mmol_c/L$.

The sodic solutions are prepared using sodium chloride (NaCl) and calcium chloride dihydrate ($CaCl_2 \cdot 2H_2O$). Table 2 summarizes the concentrations in mg/L or mmol/L used to prepare each sodic solution (Table 2). For each sodic solution, 40 ppm $HgCl_2$ was added to inhibit biological activity (McNeal and Reeve, 1964).

Table 1
Initial physicochemical characteristics of the studied soil samples

Physicochemical characteristics of soil samples								
Soil particle size (%)			Soil chemical characteristics					
Clay (<0.002 mm)	Silt (0.002–0.05 mm)	Sand (0.05–2 mm)	ESP	CEC $cmol_c Kg^{-1}$	$CaCO_3$ (%)	pH	EC (dS m^{-1})	OM (%)
47	39	14	11.63	18.6	19.5	8.01	1.97	2.22

Source: Laoufi (2010)

Table 2
SAR values obtained from different concentrations of NaCl and $CaCl_2$,$2H_2O$

SAR	Saline concentrations			
	NaCl ($mmol_c l^{-1}$)	$CaCl_2 \cdot 2H_2O$	NaCl ($mg\ l^{-1}$)	$CaCl_2 \cdot 2H_2O$
0	0	20	0	1470
5	10.75	9.24	628.87	679.14
10	15.31	4.68	895.92	343.98
15	17.33	2.66	1013.8	195.53
20	18.32	1.68	1071.72	123.48
25	18.97	1.03	1109	75.70
30	19.18	0.82	1122	60.27

2.3. Soil hydraulic conductivity measurement

2.3.1. Status of samples prior to soil hydraulic conductivity measurement

Before measuring hydraulic conductivity, it is worth noting that the soil material was used solely to apply the various exchange site saturation treatments with Na+ and Ca2+ at a constant salt concentration of 2 dS m^{-1}. Thus, the most important characteristics (clay texture and mineralogy) that can affect the physical behavior of the soil will remain constant. Regarding OM, in the experiment, we add $HgCl_2$ to all saline and sodic solutions to inhibit all biological activity, which can affect the soil structure, as the aim is to assess the effect of sodium/calcium on physical properties only. Regarding $CaCO_3$, even though the soil is saturated, calcium carbonate is a salt that dissolves slightly in the environment. In accordance with the literature, we ensure that the pore volume is sufficient to create a suitable equilibrium between the salt solution and the adsorption complex, as evidenced by changes in EC measured during soil saturation with various salt solutions, as described in Materials and Methods. In this type of experiment, we require 10 to 15 volume pores to establish a new equilibrium between the soil and the salt solution (Curtin et al., 1994). Overall, we aimed to control as many factors as possible that would affect the physical behaviour of the soil sample, and leave only the dynamic soil physical properties (soil structure and SHC).

2.3.2. Soil hydraulic conductivity measurement process

Saturated hydraulic conductivity was measured in the laboratory using a constant head permeameter (Fig. 1). According to Fadl (1979) and Luo et al. (2020), laboratory measurements of Ks are subject to two types of errors: the boundary effect, which creates a preferential flow of percolating water at the soil-permeameter interface, and the destruction of soil structure during the grinding and sieving of soil samples. The first type of error can be mitigated using the modified permeameter (Fig. 1) de-

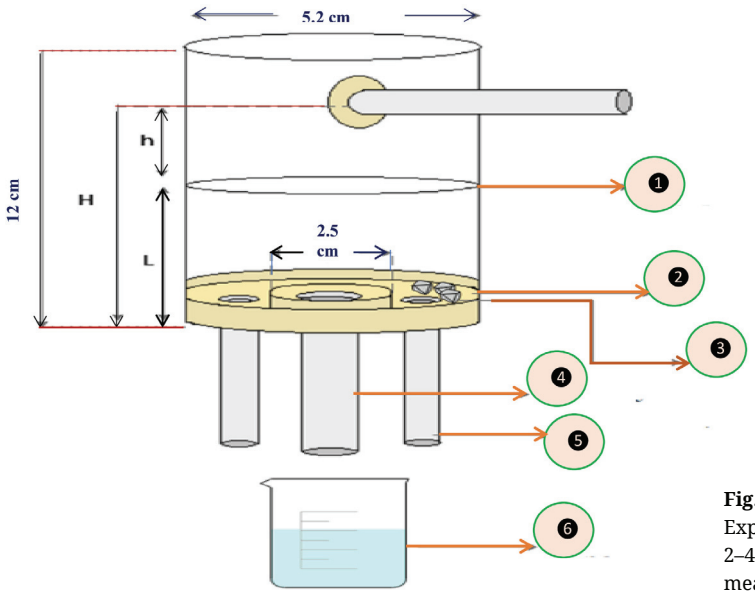

Fig. 1. Schematic diagram of the permeameter (McNeal et Reeve, 1964). Explanations: (1) Filter paper; (2) Nylon mesh; (3) Decalcified gravel of 2–4 mm; (4) Inner outflow; (5) Outer outflow and (6) Beaker for volume measurement from inner region

veloped by McNeal and Reeve (1964), and the second type can be minimized by implementing specific precautions when filling the soil sample to the desired bulk density in the permeameter. Furthermore, the flow through the inner region of the permeameter was utilized to measure the SHC. In contrast, the flow through the outer and inner regions was employed to monitor the equilibrium of the soil solution with the percolating solution. A nylon mesh screen was affixed to the top of the soil sample to prevent the disturbance of the soil particles during the experiment. A constant hydraulic gradient of approximately three was maintained throughout the measurements.

The samples were subsequently wetted from the top by applying salt solutions of appropriate electrical conductivity (EC) and sodium adsorption ratio (SAR) to their surfaces (see chapter 2.2.). A total of 21 solutions with identical EC values but varying SAR (Table 2) were then sequentially applied to the sample under three distinct scenarios:

- Scenario 1 (SAR Increment of 5: gradual increase/decrease in sodicity (0, +5, +10, +15, +20, +25, +30, and then –25, –20, –15, –10, –5, 0)
- Scenario 2 (SAR increment of 15**):** Moderate increase/decrease in sodicity (0, +15, +30, and then 0, –15, 0);
- Scenario 3 (SAR increment of 30**):** abrupt increase/decrease in sodicity (0, +30, then 0).

Each SAR treatment level was assessed in triplicate (n = 3), with independent permeameter columns constructed for each replicate. This approach yielded a total of 63 experimental units throughout the study (7 SAR levels × 3 scenarios × 3 replicates for the increasing phase, in addition to corresponding measurements for the decreasing phase).

Prior to the accurate measurement of the Ks, a predetermined number of pore volumes of each solution were passed through the soil samples. The flow rate and electrical conductivity (EC) were monitored at regular intervals to achieve both chemical equilibrium (where EC remained constant over time) and physical equilibrium (where the flow rate remained constant). In fact, the physical equilibrium time (Table 3) has been considered as the decisive criterion for an accurate and relevant measurement of SHC. Moreover, the desodification phase was achieved by reversing the SAR sequence while maintaining a constant EC at 2 $dS.m^{-1}$. Solutions for decreasing SAR were prepared by progressively increasing the $CaCl_2$, $2H_2O$ concentration while decreasing NaCl concentration (Table 2). This promoted Ca_c^{+}-Na^{+} exchange on clay surfaces, with sodium being displaced from exchange sites and removed in the effluent. The same equilibration protocol (11–16 pore volumes) was applied to ensure complete ion exchange before Ks measurements were taken. The objective of the experiment, in reverse order, by decreasing the sodium adsorption ratio (SAR) to its original value SAR 0, was to measure the hysteresis effect on any changes in hydraulic conductivity by decreasing the SAR to its original value, SAR 0.

2.4. Experimental set-up description: McNeal and Reeve permeameter

The permeameter was constructed using acrylic resin tubing. The apparatus comprises a percolating tube with an inner diameter of 5.2 cm and a height of 12 cm, featuring a 10 cm hole to establish a steady-state hydraulic gradient. At the base of the tube, a concentric circle (inner diameter of 2.5 cm, hole of 1.04 cm) is affixed with epoxy resin, which facilitates the measurement of Ks. The outer region features two lateral holes, each with a diameter of 0.65 cm, which serve to mitigate the boundary flow error during measurement. A nylon mesh was affixed to the bottom, and a layer of decalcified gravel (2–3 mm in diameter) was incorporated at the base to prevent hole formation.

2.5. Soil sample preparation for saturation with the different sodic solutions

Soil samples were dried and sieved to a 1 mm mesh size (McNeal and Reeve, 1964). The mass of the soil sample was 54.657 g with a bulk volume of 53.066 cm^3. The total mass was divided into four portions, which were carefully introduced into the permeameter to a height of 2.5 cm, achieving a bulk density of 1.03 g cm^{-3} (McNeal et al., 1968). A filter paper was placed above the soil surface samples to prevent disturbance of soil particles during the saturation process and Ks measurements.

The saturation of soil samples was determined using the concept of pore volume. The pore volume of the solution is defined as the volume of solution that the soil contains at saturation and is calculated by multiplying the porosity of the soil by the volume of soil packed in the column (Lahlou et al., 1998; Klopp and Daigh, 2019).

The pore volume was calculated using the relationship between the total porosity, bulk density, and particle density as follows:

$$PT\ (\%) = (1 - \frac{Da}{Dr}) \times 100 \qquad \text{Equation 2}$$

Where:
PT – the total porosity (%), Da – the bulk density (g cm^{-3}), and Dr – the particle density (g cm^{-3})

In this experiment, the particle density of the soil sample

Table 3
Time required for chemical (EC) and physical (flow rate) equilibrium

Scenario	Pore Volumes	Duration of the experiment for each scenario	Equilibrium Criteria
±5	11–14	24 hours to 3 days	EC variance <5%; Flow rate variance <10%
±15	14–16	6 hours to 20 hours	Same as above
±30	11–16	4 hours–15 hours	Same as above

was determined to be 2.65 g cm^{-3}, while the bulk density was 1.03 g cm^{-3}. Using Equation 2, the total porosity of the soil sample was calculated as 61.13%. Given that the bulk volume of the soil sample is approximately 53.066 cm^3, one pore volume is equivalent to 32.43 cm^3 or 32.43 mL.

The equilibrium between the soil sample and various saline solutions was monitored by adding a specific number of pore volumes. According to the literature, steady-state equilibrium between the soil solution and adsorbent complex is achieved between 10 and 15 pore volumes (Curtin et al., 1994; Levy et al., 2005). In this experiment, 11 and 16 pore volumes percolated prior to the measurement of Ks.

2.6. Darcy law to measure saturated hydraulic conductivity

After equilibrium was attained, a hydraulic gradient (approximately 3) was established using an inverted volumetric flask, and the time required for a known volume of the solution to percolate through the soil sample was recorded.

The Ks was calculated using Darcy's law as follows:

$$Ks = Q \times {}^{L}/_{A} \times (h + L) \quad \text{Equation 3}$$

Where:
Ks (cm h^{-1}) – the saturated hydraulic conductivity, Q (cm^3) – the flow rate, L (cm) – the height of the soil sample, including the gravel layer (3 cm), h (cm) – hydraulic head of 7 cm, and A – the cross-sectional internal area (4.90 cm^2).

Each measurement was performed in triplicate at a constant temperature (22°C).

2.7. Statistical analysis

The standard error of the mean (SEM) was calculated for each SAR level at a 95% confidence interval using $SEM = \frac{\sigma}{\sqrt{n}}$, where σ is the standard deviation, and n is the number of replicates (3). The 95% confidence interval was determined by multiplying the SEM by the t-value ($t_1 - \alpha/2$) for n-1 degrees of freedom (Saville and Rowarth, 2008).

One-way analysis of variance (ANOVA) was conducted on the dataset, with multiple comparisons of means using the Newman-Keuls test at a 5% significance level, as determined by SPSS software. For pairwise comparisons, the Least Significant Difference (LSD) was calculated as: $LSD = (SEM1 + SEM2) \times t1 - \alpha/_2 \times \sqrt{2}$, where SEM1 and SEM2 are the standard errors of the means being compared, and t is the Student's t-statistic at 95% confidence interval (α = 0.05) with 2(n-1) degrees of freedom (Dagnelie, 1982).

3. Results and discussion

3.1. Saturated hydraulic conductivity change as a function of increasing SAR: implications for the critical threshold soil structure degradation

The impact of increasing the SAR on Ks was evaluated using three increment scenarios: +5, +15, and +30. The results are summarized in Table 4.

Our findings reveal that the highest mean Ks values were observed at SAR 5 (2.28 ± 0.52 cm h^{-1}) for the +5 increment scenario, and at SAR 0 for the +15 (2.28 ± 0.78 cm h^{-1}) and +30 (1.89 ± 0.35 cm h^{-1}) increment scenarios. Conversely, the lowest Ks values were consistently found at SAR 30, with values of 0.51 ± 0.39 cm h^{-1}, 0.83 ± 0.57 cm h^{-1}, and 0.85 ± 0.30 cm h^{-1} for the +5, +15, and +30 increment scenarios, respectively. Moreover, ANOVA revealed significant effects of SAR level on Ks for all increment scenarios ($F_{6,14} = 14.6896$, $p = 0.000025$ for +5 increment; $F_{2,6} = 10.8200$, p = 0,010229 for +15 increment; LSD = 0.66 for +30 increment).

A significant decrease in Ks was observed between SAR 10 and SAR 15, particularly in the +5 increment scenario. Ks dropped from 1.79 ± 0.46 cm h–1 at SAR 10 to 1.16 ± 0.57 cm h–1 at SAR 15, a 35.2% reduction. This suggests a critical threshold at which the soil structure begins to degrade substantially, corroborating findings from previous studies (McNeal and Coleman, 1966; Ben-Hur et al., 2009).

Table 4
Saturated hydraulic conductivity values (cm h^{-1}) at increasing SAR under the three different scenarios (+5, +15, +30)

Values of SAR	Increments		
	+5	+15	+30
0	2.06a± 0.05	2.28a±0.78	1.89a±0.35
5	2.28a±0.52		
10	1.79a±0.46		
15	1.16b±0.57	1.68b±0.53	
20	0.77b±0.75		
25	0.73b±0.37		
30	0.51b±0.39	0.83b±0.57	0.85b±0.30

Explanation: a and b: values of Ks with different value means there is a statistical significance at a threshold of 0.05

3.2. General trend of Ks with increasing SAR

A consistent decrease in Ks was observed as SAR increased from 0 to 30 across all increment scenarios. In the +5 increment scenario, Ks decreased from 2.06 ±0.05 cm h^{-1} at SAR 0 to 0.51 ±0.39 cm h^{-1} at SAR 30, representing a 75.2% reduction. The +15 increment scenario showed a decrease from 2.28 ±0.78 cm h^{-1} to 0.83 ±0.57 cm h^{-1} (63.6% reduction), while the +30 increment scenario exhibited a decrease from 1.89 ±0.35 cm h^{-1} to 0.85 ±0.30 cm h^{-1} (55.0% reduction).

An exception to this trend was noted at SAR 5 in the +5 increment scenario, where Ks increased slightly from 2.06 ±0.05 cm h^{-1} at SAR 0 to 2.28 ±0.52 cm h^{-1}, a 10.7% increase. This anomaly can be explained by the saturation method (flooding) employed, which may have caused the release of entrapped air during the percolation of the sodic solution, temporarily increasing the porosity (Moutier et al., 1998).

3.3. Relative hydraulic conductivity analysis

To better quantify the rate of change in Ks as a function of increasing SAR, we calculated the relative hydraulic conductivity (Ks-rel) by dividing each Ks value by the reference Ks value at SAR 0 (Ks0). The results are shown in Fig. 2.

The magnitude of the change in Ks-rel varies according to the SAR increment scenario. In the +5 increment scenario, Ks-rel decreased from 1.0 at SAR 0 to 0.25 at SAR 30, a 75% reduction. The +15 increment scenario showed a decrease from 1.0 to 0.36 (64% reduction), while the +30 increment scenario exhibited a decrease from 1.0 to 0.45 (55% reduction).

The most pronounced decrease in Ks-rel was observed in the +5 increment scenario, particularly between SAR 10 and 20, where Ks-rel dropped from 0.87 to 0.37, a 57.5% reduction over this range. Conversely, the +30 increment scenario showed the least dramatic change in Ks-rel, with only a 55% reduction over the entire SAR range.

Numerous studies have demonstrated that a small, gradual increase in exchangeable sodium has a significant impact on the dispersion of clay particles, and consequently, on SHC (Lebron and Suarez, 1992; Levy et al., 1993; Aydin et al., 2004). Interparticle swelling is strongly influenced by the progression of sodicity by an increment of +5, because swelling is a continuous process that increases as sodicity increases (Keren and Ben-Hur, 2003). Increasing sodicity with the different increments used (+5, +15, +30) causes a significant decrease in the Ks of the soil sample (Table 4). This decrease was greater when sodicity increased in increment of + 5. This behavior can be explained by the fact that swelling is a continuous process that reduces the size of the conductive pores in the soil sample. Increasing sodicity by a small increment (+5) also increases the risk of dispersion of clay particles during the percolation of saline solutions (Aydin et al., 2004).

Our study makes three novel contributions to understanding sodic soil behavior. First, we systematically compared three SAR increment scenarios (±5, ±15, and ±30), revealing that the rate of sodification significantly affects the magnitude and persistence of structural changes. Second, we introduced a quantitative Hysteresis Index (HI) that enables comparison of irreversibility across different sodification-desodification pathways. Third, we found that gradual SAR changes (±5 increments) produce more severe and persistent reductions in hydraulic conductivity than abrupt changes, challenging conventional reclamation approaches that focus solely on final SAR values rather than the pathway of change.

Our findings elucidate a previously undocumented correlation between the size of sodium adsorption ratio (SAR) increments and the extent of hydraulic conductivity degradation. While classical studies have demonstrated that gradual increases in sodium levels influence clay dispersion (Quirk and Schofield, 1955; McNeal et al., 1968; Frenkel et al., 1978; Goldberg and Forster, 1990; Daoud, 1993; Keren and Ben-Hur, 2003; Levy et al., 2005), our systematic comparison of three distinct increment scenarios (±5, ±15, ±30) provides the first quantitative evidence that the sodification pathway fundamentally alters soil structural response.

Recent advancements in understanding soil hydraulic behavior under saline-sodic conditions corroborate our observations. Kramer et al. (202) introduced mathematical frameworks

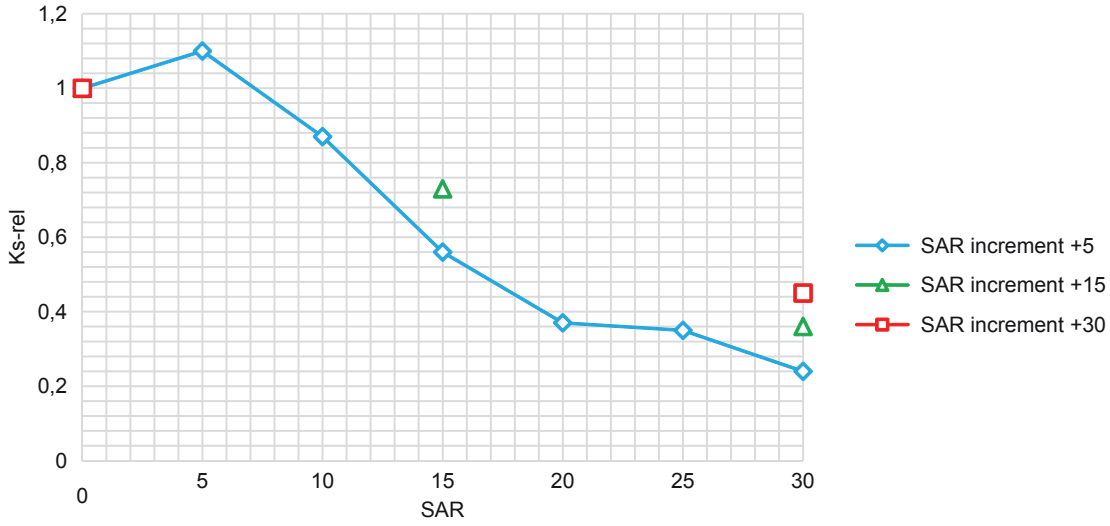

Fig. 2. K relative as a function of increasing SAR at the three different increments (+5, +15+30)

for quantifying pathway-dependent effects, demonstrating that soil hydraulic properties retain a memory of their sodification history. Our results extend this theoretical framework by providing empirical evidence that smaller SAR increments (+5) result in a 75% reduction in hydraulic conductivity (Ks), compared to only a 55% reduction with larger increments (+30), despite reaching the same final SAR value. Furthermore, our findings that interparticle swelling is more significantly influenced by +5 increments align with Klopp and Daigh's (2019) observations of non-linear hydraulic responses, uniquely demonstrating that the kinetics of sodification – not merely the endpoint – determine the severity of structural degradation.

3.4. Saturated hydraulic conductivity change as a function of decreasing SAR at three increments (–5, –15, –30)

The effect of decreasing SAR on the Ks is important for understanding the physical changes that occur when sodium replaces calcium in a fixed EC environment; the results are summarized in Table 5.

Our result shows that for the increment of decrease (–5), Ks ranged from 0.51 ±0.39 cm h^{-1} to 0.35 ±0.29 cm h^{-1}, with the highest value observed at Highest Ks observed at SAR 30, lowest at SAR 15, then for the increment of decrease (–15), Ks ranged from 0.83 ±0.57 cm h^{-1} to 0.41 ±0.34 cm h^{-1}, with the highest Ks observed at SAR 30, lowest at SAR 0, finally, For the –30 decrement scenario, Ks ranged from 0.85 ±0.30 cm h^{-1} to 0.71 ±0.33 cm h^{-1}, Highest Ks observed at SAR 30, lowest at SAR 0. ANOVA showed no significant effect of decreasing sodium, irrespective of the increment ($F_{6,14}$ = 0,49284, p = 0,803325for –5 increment; $F_{2,6}$ = 2,31724, p = 0,179599 for –15 increment; LSD = 0,63 for –30 increment), and the lack of a significant change in Ks with decreasing SAR suggests that the soil structural changes induced by high sodium levels are not readily reversible in the short term. This observation is consistent with the findings of Marchuk and Rengasamy (2012), who reported that soil structural deterioration due to sodicity can persist even after leaching of excess sodium.

The persistently low Ks values, even as the SAR decreased, suggested that the soil structure remained degraded. This could be due to the formation of stable microaggregates during the sodification process, which are not easily disrupted by subsequent decreases in SAR (Baumgartl and Horn, 1991). In conclusion, these results showed that the addition of calcium in increments of +5, +15, and +30 did not significantly improve the Ks of the soil sample under non-saline conditions.

3.5. Evaluation of the reversibility of Ks induced by sodicity: hysteresis effect

The Ks values obtained with increasing SAR were compared to those obtained with decreasing SAR at different increments to highlight the degree of reversibility of soil structural changes and the magnitude of the difference between Ks obtained with increasing SAR and those obtained with decreasing SAR (Table 6), thereby refining the analysis. We used the LSD test with a 5% threshold probability to compare the values of Ks at increasing and decreasing values at the same SAR. The hysteresis effect was measured using a normalized metric, which is determined as follows (equation 4):

$$\mathrm{HI}\ (\%) = \frac{\text{Ks increasing} - \text{Ks decreasing}}{\text{Ks increasing}} \qquad \text{Equation 4}$$

Where:
Ks increasing – at increments 5, 15 and 30; Ks decreasing – at increments x 5, 15, 30

The index can have a value ranging from 0 to 1, and whenever the value of the index approaches 1, it indicates a high hysteresis between the two values of Ks at increasing and decreasing SAR.

The data presented in Table 1 demonstrate the reversibility of Ks under the various SAR increment scenarios. The ±15 and ±30 increment scenarios exhibited significant differences between increasing and decreasing SAR values, albeit with reduced magnitudes compared with the ±5 scenario. For example, in the ±30 increment scenario, the difference (1.18) remains significant (LSD = 0.69, S), but is notably smaller than the initial difference in the ±5 scenario (1.66). This observation further supports the trend of diminishing the hysteresis in larger increments. The ±5

Table 5
Saturated hydraulic conductivity values at decreasing SAR under the three different scenarios (–5, –15, –30)

Values of SAR	Increments		
	–5	–15	–30
30	0.51a±0.39	0.83a±0.57	0.85a±0.30
25	0.55a±0.30		
20	0.59a±0.58		
15	0.35a±0.29	0.53a±0.29	
10	0.39a±0.18		
5	0.38a±0.15		
0	0.40a±0.18	0.41a±0.34	0.71a±0.33

Explanation: a and b: values of Ks with different value means there is a statistical significance at a threshold of 0.05

Table 6
Comparison of saturated hydraulic conductivity (Ks) for increasing and decreasing Sodium Adsorption Ratio (SAR) at the three scenarios

Scenario	Increment	Increasing SAR	Decreasing SAR	SARinc – SARdec	LSD (5%)	HI (%)
(1) +/–5	±5 Increment					
	0	2.06 ±0,02	0.40±0.06	1.66	0.24 **(S)**	0.807443
	+/–5	2.28±0.17	0.38±0.05	1.90	0.66 (S)	0.834795
	+/–10	1.79±0.15	0.39±0.06	1.40	0.63 **(S)**	0.782528
	+/–15	1.16±0.19	0.35±0.10	0.81	0.87 **(NS)**	0.686782
	+/–20	0.77±0.25	0.59±0.20	0.18	1.35 **(NS)**	0.242424
	+/–25	0.73±0.12	0.55±0.10	0.18	0.66 **(NS)**	0.376712
(2) +15/–15	±15 increment					
	0	2.28±0.26	0.41±0.10	1.87	1.08 **(S)**	0.81
	+15/–15	1.68±0.18	0.53±0.11	1.15	0.87 **(S)**	0.68
(3) +/–30	±30 increment					
	0	1.87±0.12	0.71±0.11	1.18	0.69 **(S)**	0.62

Explanations: S: significant difference at a threshold of 0.05, NS: non-significant difference at a threshold of 0.05, and (1), (2), (3) symbolize the three scenarios.

increment scenario exhibited a strong hysteresis effect in the first three increments (0, +/–5, +/–10). The difference between the increasing and decreasing SAR (SARinc – SARdec) is statistically significant (S) in these cases. However, as the increments increased to ±15 and above, the hysteresis effect became less pronounced and statistically non-significant (NS).

In the ±15 increment scenario, we observed a significant hysteresis effect for both increments tested (0 and +15/–15). This suggests that the soil exhibits a memory of its sodification history, even at larger increments. The ±30 increment scenario also showed a significant hysteresis effect, although the magnitude of the difference between the increasing and decreasing SAR was smaller than that of the lower increment scenarios.

3.6. Hysteresis index analysis

In the ±5 increment scenario, a strong hysteresis effect (HI > 0.75) was observed in the first three increments (0, +/–5, +/–10). This suggests that, at lower SAR levels, the soil exhibits a significant memory effect (Fig. 3).

As the increments increased in the ±5 scenario (+/–15, +/–20, +/–25), HI decreased, indicating a reduction in the hysteresis effect. This could imply that at higher SAR levels, the soil behavior became more reversible. The ±15 increment scenario shows a strong hysteresis effect for both tested increments, with HI values above 0.68. This indicates that, even at larger increments, the soil retains a significant memory of its sodification history.

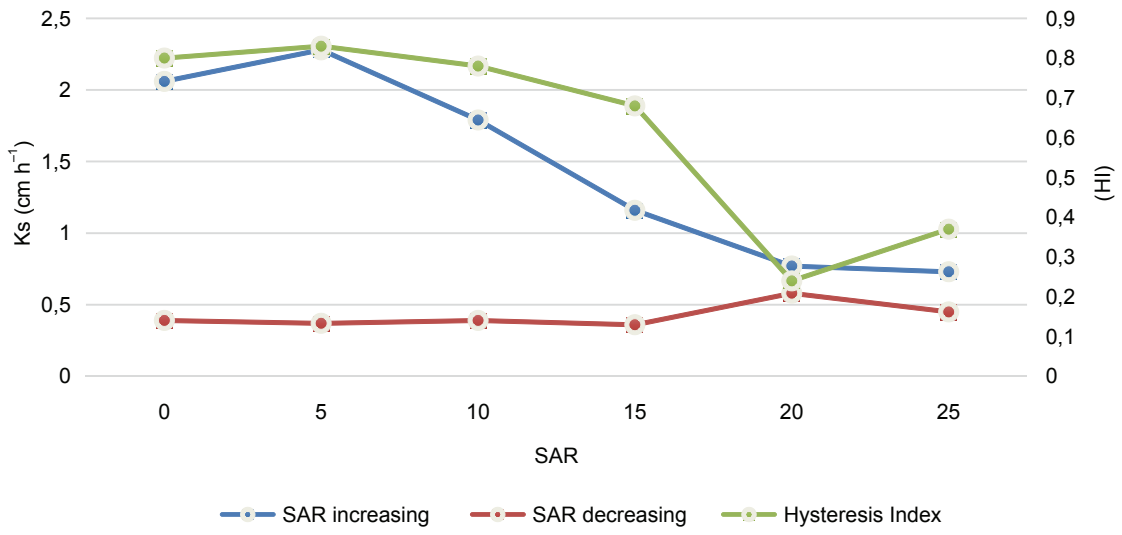

Fig. 3. Hysteresis in saturated hydraulic conductivity (Ks) for ±5 increment

The ±30 increment scenario also showed a substantial hysteresis effect (HI = 0.6203), although it was somewhat lower than the effects observed at smaller increments.

Our results reveal a consistent pattern where increasing SAR values exceed decreasing SAR values across all scenarios, indicating pronounced hysteresis in SHC dynamics. This effect was particularly evident in the ±5 increment scenario, where initial Ks values (2.06 ± 0.02 cm h^{-1}) were significantly higher than corresponding decreasing SAR values (0.40 ± 0.06 cm h^{-1}). These findings align with recent work by Adeyemo et al. (2022) and extend earlier observations by McNeal and Coleman (1966) regarding the irreversible nature of hydraulic conductivity changes in sodic soils.

The magnitude of hysteresis showed clear dependence on increment size. In the ±5 increment scenario, the difference between increasing and decreasing SAR values (SARinc-SARdec) decreased systematically from 1.66 at the initial stage to 0.18 at the ±25 increment. This trend suggests that larger fluctuations in soil sodium levels may reduce hysteresis. This finding adds nuance to our understanding of soil structural dynamics as described by Bennett et al. (2016).

Our results indicate two primary mechanisms controlling structural changes, supporting previous findings (Quirk, 2001; Dane and Klute, 1977; Mitchell and Donovan, 1991). The swelling mechanism appears to be reversible, whereas particle dispersion and subsequent pore clogging lead to irreversible changes under our experimental conditions. This distinction is particularly evident in the statistical significance patterns observed across different increment scenarios. For instance, in the ±5 increment scenario, significant differences ($p < 0.05$) between increasing and decreasing SAR values were observed for the first three increments (0, +/–5 and +/–10), suggesting dominant clay swelling effects. However, as increments increased to ±15 and above, the differences became non-significant, indicating a transition to dispersion-dominated processes (Dane and Klute, 1977). While clay swelling is generally considered reversible in principle (Dane and Klute, 1977), our results demonstrate that under specific conditions—particularly at low salinity (2 dS m^{-1}) with gradual SAR increments—even swelling-induced changes can exhibit significant hysteresis. This suggests that the theoretical reversibility of swelling may be compromised by concurrent micro-scale particle rearrangements that create quasi-permanent structural modifications.

The observed hysteresis can be comprehended through the framework proposed by Adeyemo et al. (2022) concerning Ksat reversibility under variations in salinity-sodicity. They identified clay swelling (reversible) and clay dispersion (largely irreversible) as the primary mechanisms, with dispersion becoming predominant in soils with high clay content (≥40%). Our clay-rich soil (47% with interstratified smectite-illite) exhibited persistent hysteresis across all SAR increment scenarios (HI > 0.62), corroborating Adeyemo et al.'s prediction that clay dispersion predominates in such soils, thereby limiting Ksat rehabilitation. Furthermore, our observation that smaller increments result in higher hysteresis (HI = 0.81 for ±5 vs. HI = 0.62 for ±30) supports Adeyemo et al.'s emphasis on the sensitivity of soil structure to the rate and magnitude of changes in the (C, SAR) parameter space. This suggests that in clay-rich soils, even transient exposure to elevated SAR can induce lasting structural modifications, highlighting the necessity for preventive management strategies.

This observation underscores the delicate balance between soil solution chemistry and soil structure, emphasizing the need for careful management of irrigation water quality and soil amendments in agricultural practices. Understanding these intricate relationships can help in developing more effective strategies for maintaining soil health and optimizing water use efficiency in various soil types and environmental conditions.

4. Conclusions

The findings of this investigation provide significant insights into the complex dynamics and reversibility of soil structural changes under sodic conditions. The main aspects identified are:

- SAR-Induced changes in Hydraulic conductivity: We observed a consistent decrease in Ks as the SAR increased from 0 to 30, with the most pronounced effects occurring at lower SAR values (0–15). This trend was evident across all increment scenarios (±5, ±15, and ±30), confirming the sensitivity of soil hydraulic properties to even mild sodification.
- Critical threshold for soil degradation: A significant decrease in Ks was identified between SAR 10 and 15, particularly in the ±5 increment scenario. This suggests a critical threshold where the soil structure begins to degrade substantially, aligning with previous findings on the onset of clay dispersion and pore clogging mechanisms.
- Hysteresis Effect: Our study revealed a strong hysteresis effect in the relationship between SAR and Ks. The changes in hydraulic conductivity induced by increasing SAR are not fully reversible when SAR is decreased, particularly at lower SAR values. This hysteresis was most pronounced in the ±5 increment scenario, indicating that gradual changes in soil sodicity could lead to more persistent structural alterations.
- Increment-Dependent Responses: The magnitude of change in Ks and the degree of hysteresis varied with the size of the SAR increments. Smaller increments (±5) resulted in more pronounced and statistically significant hysteresis effects, particularly at lower SAR values. This finding underscores the importance of considering the rate of change in sodicity when assessing soil structural degradation.
- Implications for Soil Management: The observed poor reversibility of Ks, even after reducing SAR, highlights the challenges in reclaiming sodic soils. Our results suggest that preventing sodification, even at low SAR levels, is crucial for maintaining soil hydraulic properties. Traditional reclamation approaches that focus solely on reducing the SAR may not be sufficient to restore soil structure and function.

These results have significant implications for the management of soils in regions prone to sodification, such as arid and semi-arid areas or those using sodium-rich irrigation water. The

strong hysteresis effect observed suggests that soil structural changes induced by sodification are not easily reversed in the short term, thus emphasizing the need for proactive management strategies to prevent soil degradation. This knowledge is highly needed to develop more effective sodic soil management and recovery strategies, thereby ensuring long-term resource sustainability in many agricultural regions threatened by sodification worldwide.

References

Adeyemo, T., Kramer, I., Levy, G.J., Mau, Y., 2022. Salinity and sodicity can cause hysteresis in soil hydraulic conductivity. Geoderma 413, 115765. https://doi.org/10.1016/j.geoderma.2022.115765

Alperovitch, N., Shainberg, I., Keren, R., 1985. Effect of clay mineralogy and aluminum and iron oxides on the hydraulic conductivity of clay-sand mixtures. Clays and Clay Minerals 33(5), 443–450.

Awedat, A.M., Zhu, Y., Bennett, J.M., Raine, S.R., 2021. The impact of clay dispersion and migration on soil hydraulic conductivity and pore networks. Geoderma 404, 115297. https://doi.org/10.1016/j.geoderma.2021.115297

Aydin, M., Yano, T., Kilic, S., 2004. Dependence of zeta potential and soil hydraulic conductivity on adsorbed cation and aqueous phase properties. Soil Science Society of America Journal 68(2), 450–459.

Bardhan, G., Russo, D., Goldstein, D., Levy, G.J., 2016. Changes in the hydraulic properties of a clay soil under long-term irrigation with treated wastewater. Geoderma 264, 1–9.

Baumgartl, T., Horn, R., 1991. Effect of aggregate stability on soil compaction. Soil and Tillage Research 19(2–3), 203–213.

Ben-Hur, M., Yolcu, G., Uysal, H., Lado, M., Paz, A., 2009. Soil structure changes: aggregate size and soil texture effects on hydraulic conductivity under different saline and sodic conditions. Australian Journal of Soil Research 47(7), 688–696.

Bennett, J.M., Marchuk, A., Marchuk, S., 2016. An alternative index to the exchangeable sodium percentage for an explanation of dispersion occurring in soils. Soil Research 54(8), 949–957. https://doi.org/10.1071/SR15281

Bolt, G.H., 1979. Soil chemistry: B. Physico-chemical models. Elsevier Scientific Publishing Company, Amsterdam.

Curtin, D., Steppehn, H., Selles, F., 1994. Clay dispersion in relation to sodicity, electrolyte concentration and mechanical effect. Soil Science Society of America Journal 58(3), 955–962.

Dagnelie, P., 1982. Statistical theories and methods. Gembloux, Agricultural Press, 463 p.

Dane, J.H., Klute, A., 1977. Salt effect on the hydraulic properties of a swelling soils. Soil Science Society of America Journal 41(6), 1043–1049.

Daoud, Y., 1993. Contribution to the study of Cheliff plain soils: The salinization phenomenon, consequences on the physical properties of clay soils. Doctoral thesis, National Agronomic Institute, El Harrach.

Demo, A.H., Gemeda, M.K., Abdo, D.R., Guluma, T.N., Adugna, D.B., 2025. Impact of soil salinity, sodicity, and irrigation water salinity on crop production and coping mechanism in areas of dryland farming. Agrosystems, Geosciences & Environment 8, e70072. https://doi.org/10.1002/agg2.70072

Essington, M.E., 2015. Soil and water chemistry: An integrative approach. CRC Press, Boca Raton.

Ezlit, Y.D., Bennett, J.McL., Raine, S.R., Smith, R.J., 2013. Modification of the McNeal clay swelling model improves prediction of saturated hydraulic conductivity as a function of applied water quality. Soil Science Society of America Journal 77(6), 2149–2156.

Fadl, A.E., 1979. A modified permeameter for measuring hydraulic conductivity. Soil Science 128(2), 126–128.

Frenkel, H., Goertzen, J.O., Rhoades, J.D., 1978. Effects of Clay Type and Content, exchangeable Sodium Percentage, and Electrolyte Concentration on Clay Dispersion and Soil Hydraulic Conductivity. Soil Science Society of America Journal 42(1), 32–39.

Goldberg, S., Forster, H.S., 1990. Flocculation of reference clays and arid-zone soil clays. Soil Science Society of America Journal 54(3), 714–718.

Hillel, D., 2004. Introduction to environmental soil physics. Elsevier, New York.

Igaz, D., Aydin, E., Šinkovičová, M., Šimanský, V., Tall, A., Horák, J., 2020. Laser diffraction as an innovative alternative to standard pipette method for determination of soil texture classes in central Europe. Water 12(5), 1232. https://doi.org/10.3390/w12051232

Ilyes, M., Miller, R.W., Qureshi, R.H., 1993. Hydraulic conductivity of saline sodic soil after gypsum application and cropping. Soil Science Society of America Journal 57(6), 1580–1585.

Keren, R., Ben-Hur, M., 2003. Interaction effects of clay swelling and dispersion and CaCO3 content on saturated hydraulic conductivity. Australian Journal of Soil Research 41(5), 979–989.

Klopp, H.W., Daigh, A.L.M., 2019. Measured saline and sodic solutions effects on soil saturated hydraulic conductivity, electrical conductivity and sodium adsorption ratio. Arid Land Research and Management. https://doi.org/10.1080/15324982.2019.167222

Klopp, H.W., Arriaga, F., Daigh, A.L.M., Bleam, W., 2020. Analysis of pedotransfer functions to predict the effects of salinity and sodicity on saturated hydraulic conductivity of soils. Geoderma 362, 114078. https://doi.org/10.1016/j.geoderma.2019.114078

Kobza, J. et al., 2011. Jednotné pracovné postupy rozborov pôd (Uniform working procedures of soil analysis). Bratislava, 136 p. ISBN 978-80-89128-89-1.

Kramer, I., Mau, Y., 2023. Review: Modeling the effects of salinity and sodicity in agricultural systems. Water Resources Research 59, e2023WR034750. https://doi.org/10.1029/2023WR03475

Lahlou, M., Badraoui, M., Soudi, B., 1998. SMSS: software for simulating salt movement in soil. Etude et Gestion des Sols 5(4), 247–256.

Laoufi, H., 2010. Geochemical processes of soil salinization in Lower Cheliff. Master's thesis, National School of Agronomy, El Harrach.

Lebron, I., Suarez, D.L., 1992. Electrophoretic mobility of illite and micaceous soil clays. Soil Science Society of America Journal 56(4), 1106–1115.

Lebron, I., Suarez, D.L., Yoshida, T., 2002. Gypsum effect on the aggregate size and geometry of three sodic soils under reclamation. Soil Science Society of America Journal 66(1), 92–98.

Levy, G.J., Eisenberg, H., Shainberg, I., 1993. Clay dispersion as related to soil properties and water permeability. Soil Science 155(1), 15–22.

Levy, G.J., Rosenthal, A., Tarchitzky, J., Shainberg, I., Chen, Y., 1999. Soil hydraulic conductivity changes caused by irrigation with reclaimed waste water. Journal of Environmental Quality 28(5), 1658–1664.

Levy, G.J., Goldstein, D., Mamedov, I.A., 2005. Saturated hydraulic conductivity of semiarid soils: combined effects of salinity, sodicity, and the rate of wetting. Soil Science Society of America Journal 69(3), 653–662.

Levy, G.J., Shainberg, I., 2005. Sodic soils. [In:] Encyclopedia of Soils in the Environment. Academic Press, New York, 504–513.

Levy, G.J., 2011. Impact of long-term irrigation with treated wastewater on soil-structure stability—The israeli experience. Israel Journal of Plant Sciences 59(2), 95–104. https://doi.org/10.1560/IJPS.59.2-4.95

Luo, Q., Mengshi, L., Wang, T., Peng, W., 2020. Correction Method for Hydraulic Conductivity Measurements Made Using a Fixed Wall Permeameter. Mathematical Problems in Engineering 2020, 1274728, 9 p.

Mace, J.E., Amrhein, C., 2001. Leaching and reclamation of a soil irrigated with moderate SAR waters. Soil Science Society of America Journal 65(1), 199–204.

Mandal, U.K., Bhardwaj, A.K., Warrington, D.N., Goldstein, D., Bar-Tal, A., Levy, G.J., 2008. Changes in soil hydraulic conductivity, run-

off, and soil loss due to irrigation with different types of saline-sodic water. Geoderma 144(3–4), 509–516. https://doi.org/10.1016/j.geoderma.2008.01.005

Marchuk, A., Rengasamy, P., 2012. Clay behaviour in suspension is related to the ionicity of clay-cation bonds. Applied Clay Science 53(4), 754–759.

Mathieu, C., Pieltain, F., 2003. Analyse chimique des sols: méthodes choisies (Soil chemical analysis: Selected methods). Paris: Tec et Doc. Lavoisier.

McGeorge, W.T., 1954. Diagnosis and improvement of saline and alkaline soils. Soil Science Society of America Journal 18(3), 348. https://doi.org/10.2136/sssaj1954.03615995001800030032x

McNeal, B.L., Reeve, R.C., 1964. Elimination of boundary-flow errors in laboratory hydraulic conductivity measurements. Soil Science Society of America Proceedings 28(5), 713–714.

McNeal, B.L., Coleman, N.T., 1966. Effect of solution composition on the swelling of extracted soil clays. Soil Science Society of America Proceedings 30(3), 313–317.

McNeal, B.L., Layfield, D.A., Norvell, W.A., Rhoades, J.D., 1968. Factors influencing hydraulic conductivity of soils in the presence of mixed salt solutions. Soil Science Society of America Proceedings 32(2), 187–190.

Minhas, P.S., Qadir, M., 2024. Agroclimate-centric irrigation water quality guidelines. Irrigation and Drainage 73(4), 1592–1605. https://doi.org/10.1002/ird.2946

Mitchell, R., Donovan, T.J., 1991. Field infiltration of a salt loaded soils: evidence of permeability hysteresis. Soil Science Society of America Journal 55(3), 708–710.

Moutier, M., Shainberg, I., Levy, G.J., 1998. Hydraulic gradient, Aging, and water quality effect on hydraulic conductivity of a vertisol. Soil Science Society of America Journal 62(6), 1488–1496.

Mukhopadhyay, R., Sarkar, B., Jat, H.S., Sharma, P.C., Bolan, N.S., 2019. Soil salinity under climate change: Challenges for sustainable agriculture and food security. Journal of Environmental Management 238, 108–122.

Oster, J.D., Shainberg, I., 1980. Flocculation value and gel structure of sodium/calcium montmorillonite and illite suspensions. Soil Science Society of America Journal 44(5), 955–959.

Oster, J.D., Shainberg, I., 2001. Soil responses to sodicity and salinity: challenges and opportunities. Australian Journal of Soil Research 39(6), 1219–1224.

Qadir, M., Schubert, S., 2002. Degradation processes and nutrient constraint in sodic soils. Land Degradation and Development 13(4), 275–294.

Quirk, J.P., Schofield, R.K., 1955. The effect of electrolyte concentration on soil permeability. Journal of Soil Science 6(2), 163–178.

Quirk, J.P., 2001. The significance of the threshold and turbidity concentration in relation to sodicity and microstructure. Australian Journal of Soil Research 39(6), 1185–1217.

Rengasamy, P., Marchuk, A., 2011. Cation ratio of soil structural stability (CROSS). Soil Research 49(3), 280–285.

Rengasamy, P., 2018. Irrigation Water Quality and Soil Structural Stability: A Perspective with Some New Insights. Agronomy 8(5), 72. https://doi.org/10.3390/agronomy8050072

Saidi, D., 1985. Agropedological study of the Mina perimeter: Evaluation of soil physical properties. Engineering thesis, National Agronomic Institute, El Harrach, 72 p.

Saville, D.J., Rowarth, J.S., 2008. Statistical measures, hypothesis, and tests in applied research. Journal of Natural Resources and Life Sciences Education 37(1), 71–82.

Shainberg, I., Letey, J., 1984. Response of soils to sodic and saline conditions. Hilgardia 52(2), 1–57. https://doi.org/10.3733/hilg.v52n02p057

Sposito, G., 2008. The chemistry of soils. Oxford University Press, New York.

Sumner, M.E., 1993. Sodic soils: new perspectives. Australian Journal of Soil Research 31(6), 683–750.

Sumner, M.E., Naidu, R., 1998. Sodic soils: Distribution, properties, management, and environmental consequences. Oxford University Press, New York.

Tavakkoli, E., Rengasamy, P., Smith, E., McDonald, G.K., 2015. The effect of cation–anion interactions on soil pH and solubility of organic carbon. European Journal of Soil Science 66(6), 1054–1062.

US Salinity Laboratory Staff, 1954. Diagnosis and improvement of Saline and alkali soils. Agriculture Handbook No. 60, USDA, Washington DC, 160 p.

USDA, 2014. Keys to soil taxonomy. 12th ed. Washington, D.C.: United States Department of Agriculture. Available at: https://ethz.ch/content/dam/ethz/special-interest/usys/ias/grassland-sciences-dam/documents/Education/Graslandsysteme/2014_USDA_Keys_to_Soil_Taxonomy.pdf

USDA, 2017. Soil Survey Manual. Soil Survey Division Staff. Soil Conservation Service, Handbook 18, chapter 3.